Eur. Phys. J. B **36**, 627–637 (2003)
DOI: 10.1140/epjb/e2004-00017-1

THE EUROPEAN PHYSICAL JOURNAL B

Melting of ice in porous glass: why water and solvents confined in small pores do not crystallize?

J. Rault[1,a], R. Neffati[1], and P. Judeinstein[2]

[1] Laboratoire de Physique des Solides, Université Paris-Sud, Bât. 510, 91405 Orsay, France
[2] RMN en milieu orienté ESA 8074, Université Paris-Sud Bât. 410, 91405 Orsay, France

Received 17 January 2003 / Received in final form 20 September 2003
Published online 30 January 2004 –

Abstract. The melting of ice in porous glass having different distribution of pores sizes is analyzed in details. One shows that confined water crystallizes only partially and that an interface layer, between the ice crystallites and the surface of the pore, remains liquid. Properties of this non crystalline interface at low temperature is studied by NMR and DSC. Both methods lead to an interface thickness h of the order of 0.5 nm, this explains why water do not crystallize when the dimension of confinement is less than a critical length $d^* \sim 1$ nm. The variation of the melting enthalpy per gram of total amount of water with the confinement length is explained taking into account two effects: a) the presence of this layer of water at the interface and b) the linear variation of the melting enthalpy ΔH_m with the melting temperature T_m. From the data of the literature one draws the same conclusions concerning other solvents in similar porous materials. Also one points out the important role of the glass temperature T_g in preventing the crystallization of the liquids confined in small pores and/or between the crystallites and the surface of the pores.

PACS. 64.70.Dv Solid-liquid transitions – 64.70.Pf Glass transitions – 81.05.Rm Porous materials; granular materials

1 Introduction

The freezing and melting of solvent and metals in porous materials have been studied in details for more than twenty years [1–12]. In most systems it has been shown that the Thomson law, relating the pore size with the melting temperature depression, is very well verified. Despite this fact, several authors have reported two intriguing properties:

a) The melting enthalpy ΔH_m of solvents confined in porous materials is found to vary with the pore dimension and then with the melting temperature [1–5].
b) In certain experimental conditions, the confined liquid crystallizes partially or does not crystallize at all. Jackson et al. [2] found that in pores of dimension less that 4 nm, decaline and cyclohexane do not crystallize. Borel [13] observed that smearing out of the solid liquid transition was possible in small gold aggregates far below the melting temperature of infinite thick crystallites T_m^0, Veprek et al. [14] found that the diamond structure of silicon and hydrogenated silicon is unstable with respect to the amorphous phase when the crystallite size is less than 2 to 3 nm. Others examples are given in the book of Turnbull [15].

The main problem in the study of solvent crystallization in small pores is that in these systems an interfacial layer of amorphous solvent can exist in certain conditions between the solid and the solvent crystallites, this has been first demonstrated by Overloop et al. [6] by NMR for organic solvents and studied by numerical simulation by Gelb et al. [16]. All the authors working in this field did not take into account this effect when calculating the total melting enthalpy (per gram of crystallizing solvent) and using the Thomson law to determine the pore dimension. In this note one studies the melting of ice in porous glasses, having sharp or large distributions of pores sizes, by two techniques: Nuclear Magnetic Resonance (NMR) and Differential Scanning Calorimetry (DSC). These two techniques permit to estimate the exact amount of crystallizing and non crystallizing water and the variation of the melting enthalpy and temperature with the pore dimensions.

The aim of this note is to demonstrate that in the system water-porous silica glass there is a linear relationship between the enthalpy of melting (per gram of crystallizing solvents) and the melting temperature depression. This

[a] e-mail: rault@lps.u-psud.fr

Table 1. Characteristic of the Silica porous glass studied: mean value of the pore diameter d, specific surface S and porosity V.

	Porous glass	d nm	S m^2/g	V cm^3/g	V/S nm
Vycor [18–21]	N1	10.2	225	0.8	3.5
	N2	30	225	0.8	"
	N3	50	225	0.8	"
	N4	70	225	0.8	"
	N5	100	230	0.82	3.56
Gelsil [22–26]	G25	2.5	610	0.48	1.1
	G50	5	580	0.63	1
Silica based	P123a	4	500	∼0.8	1.6
SBA [27–29]	P123b	7	730	1.1	1.5

relation is explained if one takes into account the existence of a non crystalline layer at the interface and the Kauzmann temperature [17]. Finally one discuss the role of the glass transition in preventing the crystallization of confined liquids.

2 Experimental results

Two classes of silica (SiO_2) porous glass, with large distribution of pore sizes have been studied: four N glasses (Vycor N° 7930, Corning Glass) and two G glasses (Gelsil glass, Geltech), these porous materials are obtained by spinodal decomposition and then dissolution of one of the two phases. Physical properties of these materials have been studied by various authors [18–26]. A third class of porous materials (called SBA in the literature [27–29]) with narrow distribution of the pore size have also been studied, samples P123a and P123b produced by templating a silica precursor (TEOS) with Pluronic copolymers. These materials show long range two dimensional hexagonal order [29]. The mean dimension d of the pores, the specific surface S and the specific volume of pore V (volume per g of material) of these porous glass are given in Table 1, these values are determined by the classical BJH (Barrett, Joyner, Halenda) method based on the analysis of the N_2 absorption isotherms.

The porous glasses have been placed in an oven with an atmosphere having 100% relative humidity with deuterated water at 25 °C; by weight measurements one verifies that after one week saturation is obtained. The samples filled with D_2O have been studied by deuterium NMR and by DSC.

2.1 NMR results

NMR experiments were performed with a Bruker AM250 spectrometer equipped with a 5 mm broad band probe without field/frequency lock control. ^{2}H NMR spectra were recorded at a frequency of 38.376 MHz. The free induction decays (FID) were recorded using a $\pi/2$ pulse width (14 μs) and a recycle delay of 2 s. 400 transients were usually added to obtain spectra with a good signal to noise (S/N) ratio. The FID signals were typically sampled with 4 K real data points over a 20 kHz spectral width and an exponential line broadening of 5 Hz was used (which is small compared to the experimental linewidth). Peak areas and line widths were obtained by deconvolution with one (or two) Lorentzian shaped curve. T_1 values were obtained by the inversion-recovery method (delay $-\pi - \tau - \pi/2$ acq.)$_n$ using 12 different τ values to obtain the T_1 following standard procedures [30]. Temperature was controlled in the range 200−300 K by a Bruker VT100 system (±1 °C regulation). Calibration was performed before each set of measurements in using the standard procedure with a reference methanol sample.

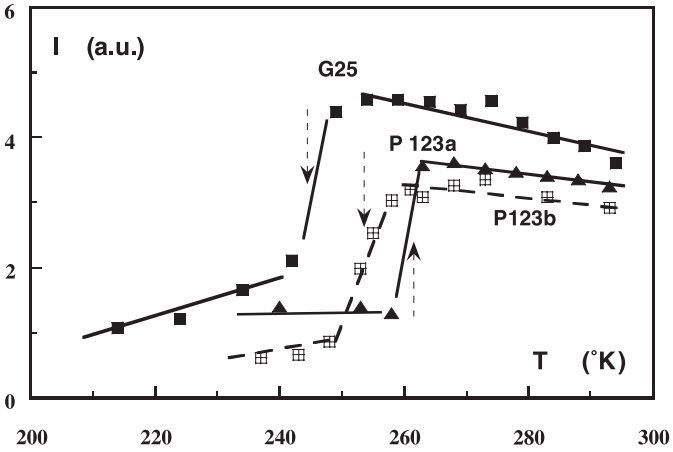

Fig. 1. Variation of the area of the ^{2}H NMR peak with temperature for deuterated water in porous glasses G25 and P123a, b of different pores sizes (see Tab. 1). Heating experiments, time between two measurements 15 min, acquisition time 15 min.

NMR intensity

The variation of the total intensity of the ^{2}H NMR peak as function of temperature is given in Figure 1 for the swollen sample G25, and the P123 samples as example. The samples were rapidly cooled to 240 K and then the spectra were acquired on heating. In these heating experiments the time between two measurements is of the order of 15 min and the acquisition time is constant 15 min (400 scans). The integrated intensity presents a sharp jump ΔI in a temperature domain of a few degrees when the ice crystallites melt, this temperature is indicated by an arrow in the figure. The accuracy on the temperature of melting T_m defined as the temperature corresponding to the jump $\Delta I/2$ is of the order of ±2 °C. This temperature is about 2 to 3 °C below the melting temperature of ice observed by DSC (temperature corresponding to the maximum of the endotherm peak obtained at 5 °C/min). At low temperature the signal intensity is weak but non zero, indicating that in the "frozen state" some "liquid" water still exist in the pores, in others words all the water do not crystallize when the temperature decreases below the crystallization temperature, a waiting time of about one hour at 220 K

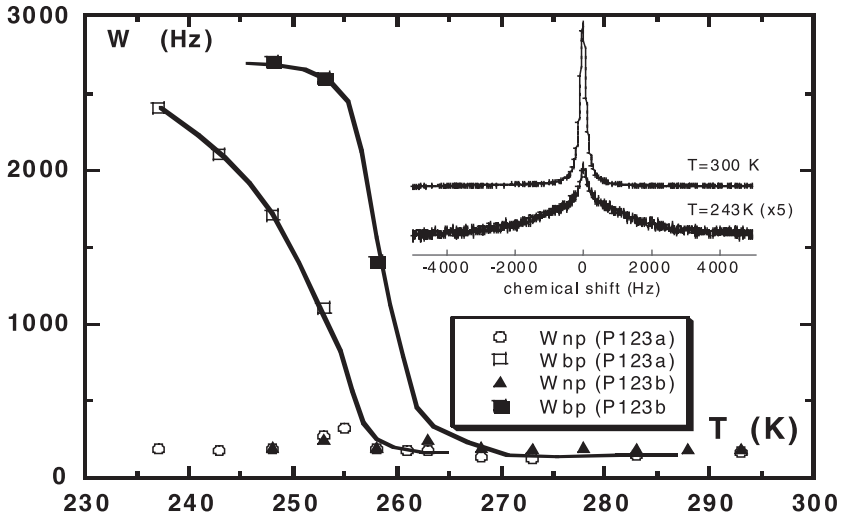

Fig. 2. Line widths W_{bp} and W_{np} of the broad and narrow NMR peaks of deuterated water in porous P123a and P123b samples. In the insert the NMR line of sample b is presented for temperatures 300 and 243 K. The central sharp peak observed at 243 K is due to bulk water, it represent 5% of the total water absorbed by the sample.

do not change this intensity. At high temperature the total intensity decreases with increasing temperature as in bulk water; this is the Curie law. One call I_{NC} and I_T the intensity just below and above the transition, the ratio I_{NC}/I_T gives the amount of non crystallizable water, m_{NC} and m_T being the mass of non crystallizable water and of total water in the sample, one writes that the amount of non crystallizable water is:

$$I_{NC}/I_T = m_{NC}/m_T \approx Sh/V \qquad (1a)$$

where h is the thickness of the water interface between the crystallites of ice and the solid glass walls. One have assumed that the non crystallized water is located in the pores and not outside of the sample for example on the surface of the glass grains. Also one has assumed that the density does vary conspicuously as function of temperature and of the distance from the interface. For the three samples, G25, P123a and P123b of Figure 1 the ratio I_{NC}/I_T is respectively equal to 0.36, 0.23, 0.30. Then knowing the ratio S/V (Tab. 1) the thickness h deduced from the above relation is respectively 0.44, 0.57 and 0.43 nm.

From the NMR intensity one concludes that all the water do not crystallize in these porous glass, non crystallizable water is confined at the solid-solid interface between the ice and the glass walls in a layer of thickness h of the order of 0.5 ± 0.1 nm which seems to be independent of the nature and geometry of the porous glass, independent on the pore size distribution. In Figure 1a one notes that the NMR intensity below T_m for monodisperse and polydisperse porous glass is constant, this indicates that the effect of non crystalline water in small pores of the glass with a large distribution of pore size is negligible compared to the non crystalline water in the interface layers (in the bigger pores containing crystallites). In materials with a large distribution of pore size (G25) the small decrease of the intensity when the temperature is decreased would be due to water confined in the smallest pores where there is no crystallite.

The main question which arises is then: does this water confined in the interface between ice and glass surface at a temperature below T_m (for example at -20 °C) has the same mobility as that of bulk supercooled water at the same temperature.

NMR line width

The NMR line width of samples P123 a and b are given in Figure 2 as function of the temperature (in heating experiments), similar variations are observed for the samples with large distribution of pore size. In the insert of the figure, the NMR peaks of sample b at room temperature and at 243 K (30 °C below T_m) are shown. At room temperature a narrow peak with half width $W_{np} = 85$ Hz is observed. At low temperature the NMR peak can be deconvoluted into a broad peak of width $W_{bp} = 2500$ Hz and a sharp peak of same half width W_{np}. The integrated intensity of the sharp peak is very weak about 4% of the total intensity measured at room temperature, and its width presents only a weak variation with temperature. On the contrary the broad peak presents a large variation of the line width at half height; the width W_{bp} decreases considerably when the temperature increases from $T_m - 20$ °C to T_m. Above T_m the line width W_{bp} becomes similar to the line width W_{np} of the narrow peak. The wide peak is attributed to the interface layer of low mobility and the narrow peak of weak intensity to water which has not crystallized in the smallest pores of the sample, probably because nucleation did not occur. The presence of this narrow peak of weak intensity at low temperature is not important if one is interested only in measurement of the amount of non crystallizable water, it provides however an interesting information: water in the supercooled state in the bulk state or in pores has not the abnormal behavior observed near -45 °C by some authors [31–35], (anomalies in the thermodynamic properties at the λ transition).

In sample P123a this sharp peak at low temperature is not observed, this difference is probably due to the different thermal treatments submitted to the samples [28,29].

Below T_m the different variations with T of the line width of the broad (and intense) peak and of the narrow and weak peak indicates clearly that the mobility of supercooled water in pore and at interface are very different. The fact that W_{bp} of the broad peak of water in the interface layers increases when temperature decreases indicates that the glass transition of this layer is higher than the glass transition of bulk water ($T_g = -135$ °C). This effect is well known in polymer systems; when approaching T_g the line width, which is related to the apparent transversal relaxation time, $W \approx (T_2^*)^{-1}$, increases with decreasing temperature [36–38]. In copolymers swollen with deuterated water it has been shown that the line width of the ^{2}H NMR peak varies according to the WLF law [38] (giving the relaxation time τ of the cooperative motions). Here a similar behavior is noted; the water interface between ice and silica glass (and water in very small pores) have a low mobility and then would have a higher T_g than bulk water. Gallo et al. [39] by computer simulation arrived to a similar conclusion concerning the 2–3 water layers at the hydrophilic surface of a solid; these authors claim that the T_g of these layers could be even equal to the ambient temperature, the observation of the large NMR peaks in our samples confirms that the remaining water in the interface layer has a higher T_g than in bulk and in the smallest pores in which water has not crystallized. One emphasizes that such important shift of the T_g (20 to 50 K) are observed in polymer films, of 10 to 20 nm thickness, absorbed on solid surface [40–43].

One must note that this low mobility water in the interface is observed by NMR in our experimental conditions because the NMR window is at least 10 times the width of the NMR broad peak (2000 Hz).

Spin lattice relaxation time T_1

Figure 3 shows the variations of T_1 of sample N1 (d = 10 nm) as function of the inverse of the temperature, the measurement are done during heating from 230 to 293 K. Also are reported the T_1 values of sample P123 at two temperatures, in the domain -25 °C $< T < 0$ °C the $T_1(1/T)$ curve (not represented) is just below the N1 curve. In this domain one can define for these samples an activation energy which 1.14 time that of bulk water above 0 °C. Also we have verifies that above T_m the approximation of fast motion is valid, the relaxation times T_1 and T_2 are of the same order of magnitude (T_2 being deduced from the width W_{np}, $T_2 = 1/\pi W_{np}$).

In this figure one gives also the T_1 values of D_2O in n-heptane emulsion between 13 °C and -37 °C reported by Hindman et al. [44–46] (see Tab. 1 of Ref. [46]). Their data fit exactly our data above 0 °C and complement them below T_m, where an non Arrhenian behavior is observed. It is in agreement with the recent light scattering studies on bulk water, Torre et al. [47] found that the relaxation time do not obey to the Arrhenius law but to a power law $1/(T - T_c)^2$, with $T_c = 228$ K. The correspondence between the different fit parameters T_0, T_c and T_λ (Vogel, mode coupling and lambda temperatures) deduced from the thermodynamic properties of bulk water is out the scope of this paper. Two important points must be noted:

a) in glass with a large distribution of pore (N), the experimental T_1 values are somewhat smaller than the bulk values (factor 1.2 to 2). Any anomaly or divergence at T_c or T_λ is not observed.
b) In glass with regular pore sizes (P123) a sharp transition occur at T_m.

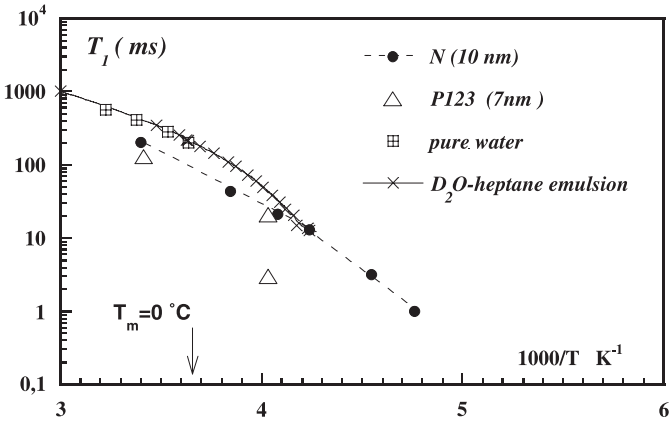

Fig. 3. Spin-lattice relaxation time T_1 of D_2O in pore and in n-heptane emulsion [44–46] as function of the inverse of the temperature. In P123b sample (triangle) the value at 250 K just below T_m, $T_1 = 20$ ms, corresponds to bulk water, 5% of water has not crystallized, and the value $T_1 = 2$ ms corresponds to the 2−3 water layers confined near the pore surface (see Fig. 2 the sharp and large NMR peaks due to these two types of water).

As discussed above, the sample P123b contains a small amount (5% of the total amount of mobile water) of free water in large pore or at the surface of the grains. T_1 of this type of water is about 2–3 times less than the value of bulk water (20–30 ms). At 250 K just below the melting temperature, the relaxation time corresponding to water which remains at the interface ice-pore surface is one order less ($T_1 = 3$ ms). It must be noted that the relation $T_1 \sim T_2$ is not observed; the assumption of fast motion is no longer valid for this type of water. This water localized between the ice crystallites and the surfaces of the porous glass (40% of the total amount of water for P123b sample for example) has a low mobility, that mean that its T_g is higher than that of bulk water.

T_1 measurements at room temperature

The relaxation time T_1 of water in the different porous glasses, measured at room temperature, is reported in Figure 4 as function of pore radius; this relaxation time verifies the following relation:

$$T_1^{-1} = (2.7 + 32/d)10^{-3} \quad (T \text{ in ms}, d \text{ in nm}) \qquad (2)$$

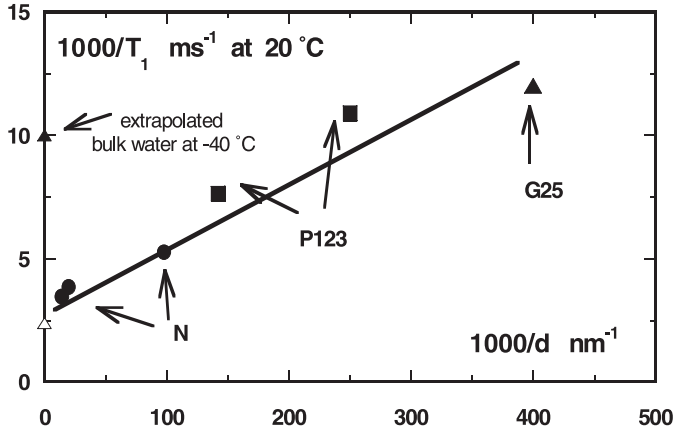

Fig. 4. Spin-lattice relaxation time T_1 of water in porous glass N, G and P123 (see Tab. 1) as function of the inverse of the pore dimension d at room temperature.

obtained by linear regression (correlation factor $\underline{R} = 0.991$). Hansen et al. [48] found similar experimental relation for others types of porous silica glasses filled with water (with large distribution of pore sizes), they shown that this relation can be explain by the "two-fraction, fast exchange" model proposed by Zimmerman and Brittin [49]. Liu et al. [3] found a similar relation for wetting organic solvents in different porous glass. In these systems the two sites fast exchange model applies. For non wetting solvent like cyclohexane in porous silica glass, these authors found a $T_1^{-1} \sim \tau_c \sim 1/d^2$ law as predicted by Korb et al. [50]. A great amount of work has been done concerning the effect of the pore size distribution and of the nature of the glass surfaces (after chemical treatment for example) on the NMR relaxation times, references are found in the paper of Liu et al. [3]. Here one wants to stress that in porous glass with sharp or large pore size distribution the relaxation time T_1 vary with d in the same way, d been determined by the BJH method. The above relation deduced from the master curve of Figure 4 can be used to determine the pore dimension of any porous material if the pore surface and the solvent have the same chemical structure. Also this relation would permit to calculate the relaxation time T_1 of water confined, in case of fast motions.

Conclusion

In conclusion the NMR results show the similarity between the various porous glass of Table 1 and the controlled pore Sigma glass studied by Overloop et al. [6], therefore water is a wetting agent for all the glass analyzed here, after crystallization in the pore there is still an non crystalline layer of water of constant thickness h between the solvent crystallites and the glass, h is of the order of 0.5 nm, this value is in agreement with the value obtained by these last authors (2.5 to 3.2 water layer) and by D'Orazio et al. [51]. These results suggest that water in pores of dimension $d^* = 2h = 1$ nm do not crystallize.

In our work and in the work of Overloop et al., one thinks that the observed decrease of mobility of water in the interface layer is due to the increase in the T_g value due to the confinement, this effect has never been noted for this type of porous materials containing crystallizing solvent. This effect of confinement on the T_g value of non crystallizable liquids in particular polymers has been widely studied [40–43] by various techniques. By broad band dielectric spectroscopy, Gorbatschow et al. [26] found that different non crystallizable derivative glycol compounds confined in nanopores present a large distribution of relaxation times, these authors using a three layer model concluded that near the solid surface solvent molecules in a layer of about 0.3 to 0.8 nm have very low mobility, it is important to remark that these organic solvents (glycol derivatives with OH groups) and water have similar bulk T_g of about -100 °C and that the so called solid like interface layers have similar thickness in silica porous glass.

In porous glass filled with water the existence of this interface layer between the solvent crystallites and the glass walls must be taken into account if one wants to measure the exact melting enthalpy of crystallizable solvent (water), if one wants to verify the Thomson law and explain why water (and the others materials; solvents and metals) in confined geometry and in form of droplet never crystallize under certain size.

2.2 DSC

DSC was performed on DSC 30 (Mettler Toledo) at slow heating rate, 2 °C/min. Typical thermograms of water confined in Gelsil and P123 glass are given in reference [41], it has been controlled that these thermograms are very similar to those obtained by the fractionated method which permits to obtain true thermograms at the thermal equilibrium [52,53]. From the maximum of the endotherm peak (heat flow vs. T) one deduces the melting temperature T_m, and the area under the heat flow curve gives the melting enthalpy ΔH_m, the amount of crystallizable and not crystallizable water can be deduced from ΔH_m, if one knows the variations of the melting enthalpy with the temperature (in most of the published work ΔH_m is assumed to be independent on T) and if the total amount of absorbed water is known with accuracy. The three families of porous glass studied in this work are compared to similar materials studied by Brun [1] and Handa et al. [5].

2.2.1 Melting temperature of confined ice

In Figure 5 the melting temperature depression $t_m = (T_m^0 - T_m)/T_m^0$ of confined ice is plotted as function of the inverse of the dimension of the pore $1/d$. T_m^0 is the melting temperature of bulk water and T_m, the melting temperature of water in the confined system. The results of Brun and Handa et al. on similar porous glass (polydispersed) filled with water, were obtained at different heating rates,

respectively 20 °C/min and 0.1 °C/min. The most important characteristic of the melting peaks of water in these various silica porous (N and G) is the important width of the endotherm peak which indicates that these systems have a large distribution of pore sizes. Recently it has been shown that the form of the melting peak, obtained at low scanning rate or by the fractionated DSC method, gives the fractal dimension of the structure in agreement with others techniques [12,52,53]. In all the samples of Figure 5 the mean dimension d values has been measured by the classical BJH method (Tab. 1). The Thomson law:

$$t_m = \left(T_m^0 - T_m\right)/T_m^0 = \frac{\beta}{d} \tag{3a}$$

has been verified for many compounds. The Thomson length β is generally written on the form:

$$\beta = \frac{4\sigma_{sl}}{\Delta H_m^0 \rho_s} \tag{3b}$$

ΔH_m^0 being the bulk melting enthalpy, σ_{sl} the solid liquid interface energy and ρ_s the density of the solid are assumed to be independent on T_m. In writing relation (3) one assumes that the melting enthalpy is independent on the melting temperature, this is not exact. The direct determination of σ_{sl} are very rare and generally this parameter is deduced from the above relation if d is known by an other technique. The Thomson length deduced from relation (3a) is of the order of 1 nm for most materials [54], water is one exception, β is of the order of 0.15 nm [1,5,12], which is of the order of the H_2O molecular size.

The fact that the different porous glass (with large and sharp pore size distribution) verify relation (3) would indicate that the thermoporosimetry and gas adsorption methods measure the same mean value of the pore size distribution function, although based on different physical phenomena. However, one must remark that the Thomson relation does not take into account the presence of the non crystalline interface layer of thickness h as in BJH method for gas adsorption. One must ask if the above relation should be replaced by the modified Thomson law:

$$t_m = \left(T_m^0 - T_m\right)/T_m^0 = \frac{\beta}{d-2h}. \tag{3c}$$

This relation was suggested by Couchman and Jesser [55]. In Figure 5 the experimental results have been fitted with equations (3), with the interface thickness $h = 0$ and $h = 0.5$ nm, the correlation factors are respectively $R = 0.985$ and 0.978, and the Thomson length $\beta = 0.15$ nm and 0.13 nm. The measurement of T_m of the different authors have been done in various experimental conditions; difference in heating rates and also in sample weights and sample forms which lead to different thermal contact in the DSC pan. Therefore one thinks that taking into account the accuracy of the determination of T_m and d, the difference in the correlation factor is not significative. In conclusion, from the Thomson laws (Rels. (3a, c)) one cannot have any direct information on the thickness of the water interface layer

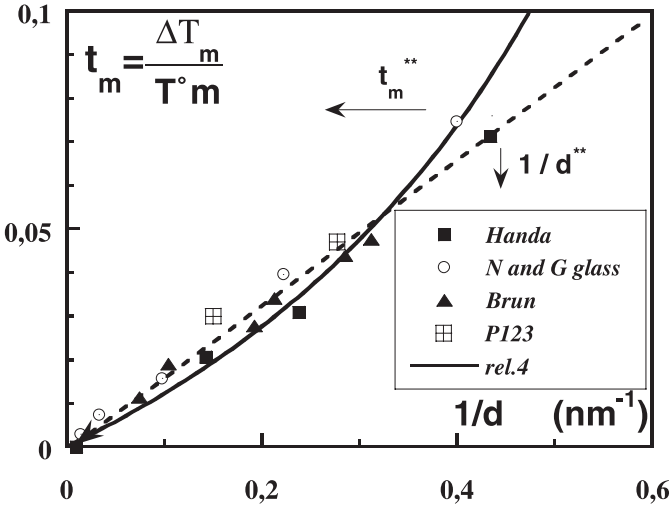

Fig. 5. Reduced melting temperature t_m of water in porous glass as function of the inverse of the pore dimension d (see Tab. 1). Heavy and dashed lines represents the best fits with the Couchman and Jesser and Thomson law (Rels. (3a, c)). Above the dimension d^{**} crystallization is not observed.

It must be noted that the Thomson law has never been verified for very small systems, $d < d^{**}$, ($d^{**} \sim 2$ nm), for the simple reason that water (and others solvents) in these systems do not crystallize. For this critical dimension, d^{**}, the corresponding melting temperature $T_m^{**} \sim -25$ °C ($t_m^{**} = 0.07$) is much higher than the glass temperature of the bulk water $T_g = -135$ °C, ($t_g = 1 - T_g/T_m^0 = 0.5$). One concludes that the viscosity of water at t_m^{**} in these small pores is much higher than in bulk water. This corroborates the NMR results, the radius $d^{**}/2$ of the critical pore is about twice the non crystallizable interface thickness h measured by NMR. For kinetics reason when $T < T_m^{**}$ any crystallite can not nucleate and grow in a reasonable time in pore of dimension $d < d^{**}$, the supercooled liquid being frozen

2.2.2 Melting enthalpy

In Figure 6 one gives the melting enthalpy of water (per gram of total absorbed water) as function of the reduced melting depression temperature t_m for the three families of porous glass studied in this work and from the works of Handa et al. [5] and Brun [1]. The important point to note is that the measured enthalpy $\Delta H_m(t_m)$ (per gram of total water) can be put on the linear form with the reduced temperature t_m

$$\Delta H_m = \Delta H_m^0 \left(1 - \frac{t_m}{t_m^*}\right); \quad t_m^* = 0.11. \tag{4}$$

In the domain $t_m^{**} < t_m < t_m^*$ crystallization is not observed. $\Delta H_m^0 = 334$ J/g is the melting enthalpy of ice of infinite size at $T_m^0 = 273$ K. The extrapolated temperature depression $t_m^* = 0.11$, ($T_m = -30$ °C) would correspond to a pore dimension $d^* = 1.5$ nm (or 2 nm) if

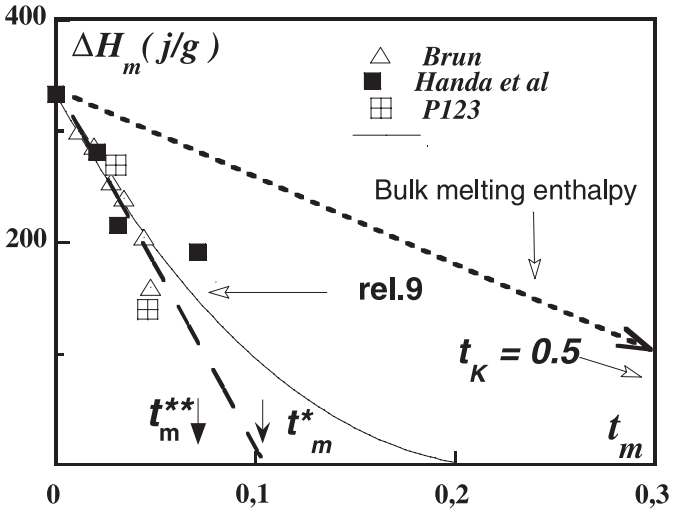

Fig. 6. Melting enthalpy ΔH_m of water per gram of total amount of water in porous glass as function of the reduced melting temperature t_m. The dashed line gives the Kauzmann variation of ΔH_m per gram of crystallizing bulk water (see Fig. 1). Continuous line gives the best fit with relation (8) and leads to a fractal exponent $D = 1.4$ of the porous structure (see text). Arrows define the critical melting temperature depressions t_m^* and t_m^{**}.

equations (3a, b) (with $h = 0.6$ nm) apply. This new empirical law is also observed for other solvents as discussed below. The origin of the extrapolated temperature t_m^* is puzzling.

In conclusion NMR and DSC measurements give the same information, the larger pore size d (measured by DSC) in which water cannot crystallize is equal to $2h$ (or of the same magnitude), twice the thickness of the non crystalline interface layer (measured by NMR). To our opinion the experimental data can fit with the same accuracy the two Thomson laws, which rely on an important assumption: the interface layer thickness h is independent on the confinement dimension d. One must wonder if the presence of the non crystalline interface layer is the only reason of the variation of the melting enthalpy per gram of total water with the reduced temperature of melting, and what is the influence of the pore size distribution.

Origin of the variation of ΔH_m with t_m and d

There are mainly two reasons for having a lower melting enthalpy of water in porous systems than in the bulk:

- The existence of a non-crystalline fraction of water (solvent) in pores at the interface ice-SiO_2 glass, generally this fraction is not taken into account by the authors in the calculation of ΔH_m.
- The decrease of the melting enthalpy when lowering the melting point, due to the differences in temperature variations of the heat capacities of the liquid and crystalline phases.

To take into account the non crystalline part of the solvent, one can estimate the ratio of the total volume of the crystallites having a typical size $d - 2h$ and of the pore with d as diameter in the following way:

$$V(d-2h)/V(d) = (1-2h/d)^D. \tag{5}$$

D depends on the shape of the pore and range between 2 (for a cylindrical pore) and 3 for a spherical one. For P123 samples with sharp cylindrical pore size $D = 2$. The measured melting enthalpy for a sharp distribution of pore size is then given by:

$$\begin{aligned}\overline{\Delta H}_m &= \Delta Hm\,(T_m)\left(1-\frac{2h}{d}\right)^D \\ &= \Delta H_m\,(T_m)\left(1-\frac{2h}{\beta}\,t_m\right)^D,\end{aligned} \tag{6}$$

where $\Delta H_m(T_m)$ gives the thermodynamic dependence of the melting enthalpy on temperature, and the second term gives the correction to take into account the non crystalline part of solvent.

In many published works the melting enthalpy of confined crystallites (per gram of crystallizing water) is assumed to be constant $\Delta H_m(T_m) = \Delta H_m^0 = 334$ J/g or slightly varying with the melting temperature [16], $\Delta H_m = \Delta H_m^0\,(T_m/T_m^0)$, with $T_m^0 = 273$ K. Since the pioneer work of Kauzmann [17] one should write ΔH_m in the form:

$$\Delta H_m(T_m) = \Delta H_m^0 \frac{T_m - T_K}{T_m^0 - T_K} = \Delta H_m^0\left(1-\frac{t_m}{t_K}\right) \tag{7}$$

with $t_K = (T_m^0 - T_K)/T_m^0$. The decrease of ΔH_m with decreasing temperature is due to the different variation of the crystal and liquid heat capacities with T. In most glass forming materials T_K is about 50 °C to 30 °C below the glass temperature T_g. (measured at 10^{-2} Hz). In many materials the empirical laws $T_K \sim T_m/2$ and $T_m \sim Tg + 100$ °C are observed [56]. At T_K the relaxation time of the cooperative α motions diverges to infinite, the comparison between the Kauzmann (T_K) and Vogel (T_0) temperatures has been given in several reviews (see for example Ref. [56]). Thus one assumes that the reduced Kauzmann temperature of water is about $t_K = 0.4$. Between T_m and T_g it has been verified that the enthalpy of the supercooled (and crystallizable) glass verifies equation (7). Then equation (6) writes:

$$\overline{\Delta H}_m = \Delta H_m^0\left(1-\frac{t_m}{t_K}\right)\left(1-\frac{2h}{\beta}t_m\right)^D \tag{8a}$$

for $t_m < \beta/2h$, the comparison with the experimental variations $\Delta H_m(t_m)$, equation (4), gives at first order:

$$\frac{1}{t_m^*} = \frac{1}{t_K} + D\frac{2h}{\beta}. \tag{8b}$$

With the experimental values: $t_m^* = 0.11$, $\beta = 0.15$ nm and $t_K = 0.4$, and $D = 2$ for cylindrical pores (P123 samples) one obtains the value $h = 0.44$ nm which is very near the value estimated by NMR. Obviously this is a crude

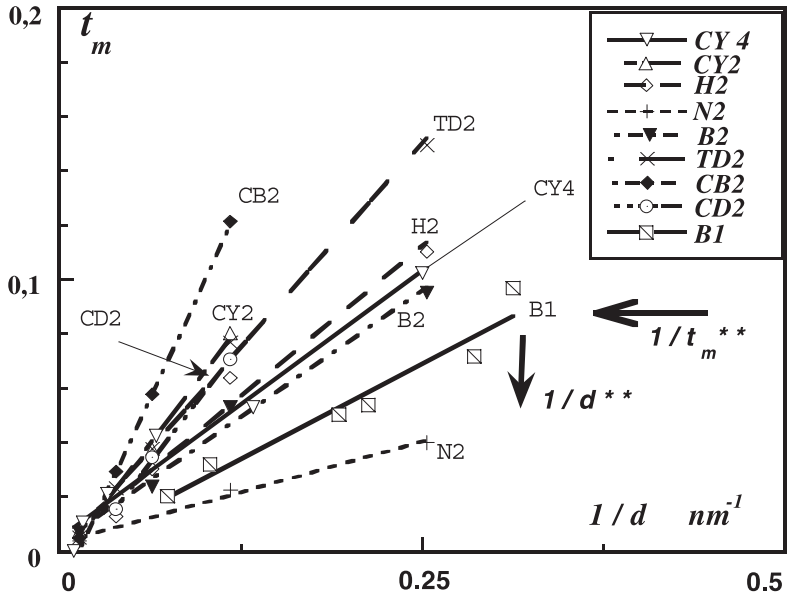

Fig. 7. Reduced melting temperature depression t_m of various organic solvents in porous glass as function of the inverse of the pore dimension d (see Tab. 2). For benzene (B1) the highest melting temperature depression observed is $t_m^{**} = 0.1$ In pores of dimension smaller than $d^{**} = 4$ nm crystallization is not observed.

estimation because the Kauzmann temperature of water deduced from the Vogel and MCT laws are not known with accuracy and also because the anomaly variation of the heat capacity observed in bulk water is not taken into account. From Figure 3 one cannot conclude that the variations of the NMR relaxation times T_1 with temperature are very different in bulk and confined states, below one stress that the others solvents which have no anomalous behavior in the supercooled state present the same effects.

As shown in reference [45], for polydispersed G porous glasses, one can postulate that the pore size distribution has the power form $P(d) \sim d^{D-1}$ then by integration $V(d) \sim d^D$. Applying relation (8) one can determine the exponent of the power law, the determination of D is however very imprecise because of the possible errors on $t_m^*(\pm 0.1)$, t_K (± 0.1) and on $h/\beta\,(\pm 0.25)$. In Figure 6, one gives however the best fit of relation (8a) with all the data of the figure corresponding to the different authors; the characteristics lengths being $h = 0.4$ nm, $\beta = 0.16$ nm and the reduced Kauzmann temperature $t_K = 0.5$, one obtains $D = 1.4$ which is not far from the fractal exponent 1.5 to 1.7 deduced from the form of the melting peak observed in the DSC thermogram and by other techniques on these types of porous glass [53]. The bad correlation coefficient ($\underline{R} = 0.9$) observed in the fit of relation (9a) impedes any precise conclusion on the form and the distribution of the pore sizes for these last series of porous glass.

3 Comparison with other solvents

The described properties of water in confined systems are not unique, organic solvents and metals also have same behavior as noted by several authors. In Figures 7 and 8 one gives the variation of t_m versus $1/d$ and ΔH_m versus t_m for organic solvents in porous glass deduced from various data reported in the literature, references are given in Table 2. The important conclusions are that as for water:

a) the Thomson law is still verified.
b) The enthalpy of melting vary linearly with the relative melting depression temperatures and extrapolates to zero for a critical value t_m^* of the melting depression temperature. This effect has never been noted.
c) In the domain $d^* < d < d^{**}$, that is to say $t_m^{**} < t_m < t_m^*$. Crystallization is not observed. The critical dimension d^{**} is dependent on the nature of the solvent, and probably on the nature of the pore surface.

For most solvents one has $0.1 < t_m^* < 0.2$. and $t_m^{**} \sim 0.8$ to $0.3\ t_m^*$. There are two exceptions: benzene in compressed Alumina ($t_m^* = 0.33$, $t_m^{**} = 0.33\ t_m^*$) and chlorobenzene ($t_m^* = 0.5$, $t_m^{**} = 0.24\ t_m^*$) in porous silica. In those cases the fact that t_m^* is about t_K could indicate, according to relation (8b), that there is no liquid interface layer ($h = 0$) between the crystallites and the pore surfaces. For all solvents the corresponding dimension of the pores d_g below which crystallization would not be observed is about 1.5 to 3 nm. One concludes that the thickness of the non crystalline layer of most of the solvents lies between 0.6 and 1.5 nm. Mu et al. [4] by DSC on cyclohexane and Gorbatschow et al. [26] by dielectric spectroscopy arrived to the same conclusion on glycol compounds in similar silica porous glass. Unfortunately for the others systems one has no data concerning the thickness h of the interface layer neither the value of the fractal exponent D, therefore relation (8) cannot be verified with accuracy.

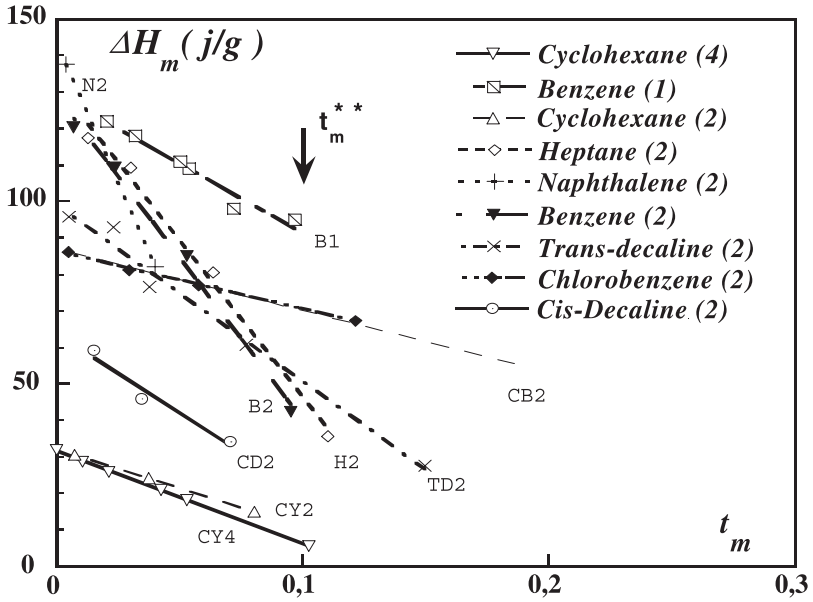

Fig. 8. Melting enthalpy ΔH_m per gram of total amount of solvent in porous glass as function of the reduced melting temperature t_m. The extrapolated values t_m^* which gives $\Delta Hm = 0$ are given in Table 2. For Cyclohexane, ΔH_m extrapolates to 0 for the Kauzmann temperature $T_K \approx 0.5T_m^0$ ($t_m^* = t_K$). The critical dimension d^{**} below which no crystallization is observed is indicated for benzene (B1).

Table 2. Critical reduced temperatures of organic solvents confined in porous glasses.

Authors (ref.)	Porous material	Solvents	t_m^*	Curves in Fig. 7 and 8.
Brun (1)	Compress	Benzene	0.33	B1
	Alumina	Water	0.09	W1
Jackson et al. (2)	Porous silica	cis-Decaline	0.14	CD2
	treated by	trans-Decaline	0.21	TD2
	trimethylsilyl	Chlorobenzene	0.5	CB2
		Naphtalene	0.1	N2
		Heptane	0.15	H2
		Cyclohexane	0.13	Cy2
Mu et al. (4)	Porous silica	Cyclohexane	0.14	Cy4
Handa (5)	Porous silica	Water	0.15	W5
Neffati (12)	Porous silica	Water	0.12	W12

4 Conclusion

In conclusion one stresses that water and other solvents confined in porous materials present the same behavior; this fact suggests that confined water present no (observable) anomalous properties as it has been reported for the bulk state (more exactly in emulsion droplets of microns size). From the DSC measurements (Rels. (3, 4)) one defines the two temperatures t_m^* and t_m^{**} (and the corresponding pore dimensions d^* and d^{**}) characteristic of the confined liquid. It is important to remark that the extrapolated characteristic melting temperature t_m^* ($\Delta H_m = 0$), Figures 6 and 8, is of the same order 0.1 to 0.2 for all the solvent (excepted for Chlorobenzene). Accurate heat capacity measurements on supercooled and confined liquids are necessary to understand the origin of this temperature, here we have suggested that this temperature is related to the Kauzmann temperature. For all the solvents the critical pore dimension d^{**} below which crystallization is not observed, is of the order of 2−4 nm, the

corresponding melting temperature depression being constant, $t_m^{**} \sim 0.1$ (excepted for chlorobenzene and benzene $t_m^{**} = 0.5$ and 0.33).

The dimension $d^{**} = 1.5$ to 2 nm for water, deduced from DSC measurements (Rels. (3, 4)) is about twice the thickness h determined by NMR. Water in pores of dimension $d^* < d < d^{**}$ do not crystallize not because the melting enthalpy decreases with T_m but because the viscosity is much higher in confined water than in the bulk. This last technique shows that water (like other solvents) confined at the interface between the solvent crystallites and the glass walls has a low mobility, indicating that the T_g of such interface is higher than that of the bulk water.

It is important to note that when a crystallite is nucleated and growth in a pore at a temperature T_c, the liquid interface between crystallite and pore surface decreases in thickness and then the mobility of the remaining liquid decreases (T_g increases). The crystallization process stops when the glass temperature of this layer becomes of the order of the crystallization temperature T_c. (the supercooling $\Delta T = T_m - T_c$ is in general of the order of 10 °C to 20 °C). In polymer and simple liquid films adsorbed on solid surfaces it is well known that the glass temperature increases with the confinement dimension, whereas T_m decreases; the intersection of the $T_m(d)$ and $T_g(d)$ curves gives the critical dimension d^{**}. This process is similar to the so called "T_g regulation process" observed in hydrophilic polymers [57,58], the effect of confinement being replaced by the effect of dilution.

In this note one has compared the behavior of water in silica porous glass having a sharp and a large distribution of pore size. Assuming that the pore size distribution verifies the power law, equation (5), one has shown that one can deduce a fractal exponent D characteristic of the porous structure if the interface thickness h and then the melting enthalpy (Eq. (8)) are known. This method is however less accurate than the method based on the analysis of the shape of the DSC heat flow curve [53].

We thank Dr. A. Davidson for stimulating discussions and for providing us the porous glass P123. Also we want to thank R. Botet for fruitful discussions.

References

1. a) M. Brun, Ph.D. thesis, University of Lyon, France (1973); b) M. Brun, A. Lallemand, J.F. Quinson, C. Eyraud, Thermochim. Acta **21**, 59 (1977)
2. C.L. Jackson, G.B. McKenna, J. Chem. Phys. **93**, 9002 (1990)
3. G. Liu, Y. Li, J. Jonas, J. Chem. Phys. **95(9)**, 6892 (1991)
4. R. Mu, V.M. Malhota, Phys. Rev. B **44**, 4296 (1991)
5. Y.P. Handa, M. Zakrzewski, C. Fairbridge, J. Phys. Chem. **96**, 8594 (1992)
6. K. Overloop, L. Van Gerven, J. Mag. Resonance A **104**, 179 (1993)
7. E. Moltz, A.R. Wong, M.H. Chan, J.R. Beamish, Phys. Rev. B **48**, 5741 (1993)
8. K.M. Unruh, T.E. Huber, C.A. Huber, Phys. Rev. B **48**, 9021 (1993)
9. B.F. Borisov, E.V. Charnaya, Y.A. Kumserov, A.K. Radzhabov, A.V. Shelyapin, Solid State Commun. **92**, 531 (1994)
10. Y.A. Kumzerov, A. Naberezmov, S.B. Vakhrushev, B.N. Sovenko, Phys. Rev. B **52**, 4772 (1995)
11. B.F. Borisov, E.V. Charnaya, P.G. Plotnikov, W.D. Hoffmann, D. Michel, Y. Kumzerov, C. Tien, C.S. Wur, Phys. Rev. B **58**, 5329 (1998)
12. R. Neffati, Ph.D. thesis, Université Paris-Sud, Orsay, France (1999)
13. J. Borel, Surf. Sci. **106**, 1 (1981)
14. S. Veprek, Z. Iybal, F.A. Sarott, Phil. Mag. B **45**, 137 (1982)
15. D. Turnbull, *Physics of Non Crystalline Solids* (Edit. Prins, North Holland, Amsterdam, 1960)
16. L.D. Gelb, K.E. Gubbins, R. Radhakrishnan, M. Sliwinska-Bartkowiok, Rep. Prog. Phys. **62**, 1573 (1999)
17. W. Kauzmann, Chem. Rev. **57**, 2680 (1948)
18. J.C. Li, D.K. Ross, J. Phys.: Condens. Matter **6**, 351 (1994)
19. J.C. Li, D.K. Ross, R.K. Heeman, Phys. Rev. B **48**, 6716 (1993)
20. U. Even, K. Rademann, J. Jortner, N. Manor, R. Reisfeld, Phys. Rev. Lett. **52**, 2164 (1984)
21. M. Arndt, F. Kremer, Mater. Res. Soc. Symp. Proc. **366**, 259 (1995)
22. P. Pissis, J. Laudat, A. Kyritsis, J. Non-Cryst. Solids **171**, 201 (1994)
23. P. Pissis, D. Daoukaki-Diamanti, L. Apekis, J. Phys.: Condens. Matter **6**, L325 (1994)
24. P. Pissis, A. Kyritsis, D. Daoukaki, G. Barut, R. Pelster, G. Nimitz, J. Phys.: Condens. Matter **10**, 6205 (1998)
25. C. Streck, Y. Mel'Nichenko, R. Richert, Phys. Rev. B **53**, 5341 (1996)
26. W. Gorbatschow, M. Arndt, R. Stannarius, F. Kremer, Europhys. Lett. **35**, 719 (1996)
27. P.T. Tanev, T.J. Pinnavaia, Science **271**, 1267 (1996)
28. Y. Bennadja, P. Beaunier, D. Margolese, A. Davidson, Microporous Mesoporous Mater. **44-45**, 147 (2001)
29. M. Imperor-Clerc, P. Davidson, A. Davidson, J. Am. Chem. Soc. **122**, 11925 (2000)
30. R.K. Harris, *Nuclear Magnetic Resonance* (Eds. Pitman, London, 1983)
31. E.W. Lang, H.D. Lüdemann, Angew. Chem. Int. Ed. Engl. **21**, 315 (1982)
32. *Water a Comprehensive Treatise*, Vol. 7, edited by F. Franks (Plenum Press, N. Y. 1981)
33. R.J. Speedy C.A. Angel, J. Chem. Phys. **65**, 851 (1976)
34. R.I. Ito, C.T. Moynihan, C.A. Angel, Nature **398**, 492 (1999)
35. E. Tombari, C. Ferrari, G. Salvetti, Chem. Phys. Lett. **300**, 749 (1999)
36. D. Hentschel, D.H. Sillescu, H.W. Spiess, Macromolecules **14**, 1605 (1981)
37. A.D. Meltzer, H.W. Spiess, Makrom. Chem. Rapid Comm. **12**, 261 (1991)
38. J. Rault, C. Macé, P. Judeinstein, J. Courtieu, J. Macromol. Sci. Phys. B **35**, 115 (1996)
39. a) P. Gallo, M. Rovere, E. Spohr, J. Chem. Phys. **113**, 11324 (2000); b) P. Gallo, M. Rovere, E. Spohr, Phys. Rev. Lett. **85**, 4317 (2000)

40. L. Keddie, R.A.L. Jones, R.A. Cory, Europhys. Lett. **27**, 59 (1997)
41. J.A. Forrest, K. Dalnoki-Veress, J.R. Dutcher, Phys. Rev. E **56**, 5705 (1997)
42. a) A. Schonhals, H. Goering, Ch. Schick, J. Non-crystalline Sol. **305**, 140 (2002); b) A. Schonhals, H. Goering, K.W. Brzezinka, Ch. Schick, J. Condens.: Matter **15**, S1139 (2003)
43. R. Richert, M. Yang, J. Phys.: Condens. Matter **15**, S1041 (2002)
44. J.C. Hindman, A.J Zilen, A. Svirmickas, M. Wood, J. Chem. Phys. **54**, 621 (1971)
45. J.C. Hindman, J. Chem. Phys. **60**, 4488 (1974)
46. J.C. Hindman, A. Svirmickas, J. Chem. Phys. **77**, 2487 (1973)
47. R. Torre, personnal communication
48. W. Hansen, C. Simon, R. Haugsrud, H. Raeder, R. Bredesen, J. Phys. Chem. B **106**, 12396 (2002)
49. R. Zimmermann, W.E. Brittin, J. Phys. Chem. **61**, 1328 (1957)
50. P. Korb, M. Winterhalter, H.M. McConnell, J. Chem. Phys. **95**, 6892 (1991)
51. F. D'Orazio, J.C. Tarczon, W.P. Halperin, K. Eguchi, T. Mizusaki, J. Appl. Phys. **65**, 742 (1989)
52. R. Neffati, L. Apekis, J. Rault, J. Therm. Analysis **54**, 741 (1998)
53. R. Neffati, J. Rault, Eur. Phys. J. B **21**, 205 (2001)
54. W. Wautelet, J. Phys. D Appl. Phys. **343**, 24 (1991)
55. P.R. Couchman, W.A. Jesser, Nature **269**, 481 (1977)
56. J. Rault, J. Non-Cryst. Solids **260**, 164 (1999) and J. Non-Cryst. Solids **271**, 177 (2000)
57. J. Rault, T. N'Guyen, R. Greff, Z. Ping, J. Neel, Polymer **36**, 1655 (1995)
58. J. Rault, Makromol. Chem., Macromol. Symp. **100**, 31 (1995)